Migration and actin protrusion in melanoma cells are regulated by EB1 protein

Joseph M. Schober[a.b.*,] Jeanine M. Cain[a], Yulia A. Komarova[c] and Gary G. Borisy[d]

a. Department of Pharmaceutical Sciences, Southern Illinois University School of Pharmacy, Edwardsville, IL 62026, USA

b. Former address: Department of Cell and Molecular Biology, Feinberg School of Medicine, Chicago, IL 60611, USA

c. Department of Pharmacology, University of Illinois College of Medicine, Chicago, IL 60612, USA

d. Marine Biology Laboratory, Woods Hole, MA 02543, USA

* Corresponding author: Joseph M. Schober

Department of Pharmaceutical Sciences

Southern Illinois University Edwardsville School of Pharmacy

220 University Park Drive

Edwardsville, IL 62026-2000, USA

Email: joschob@siue.edu

Tel: 618-650-5129

Fax: 618-650-5145

1

Abstract

Remodeling of actin and microtubule cytoskeletons is thought to be coupled; however, the interplay between these two systems is not fully understood. We show a microtubule end-binding protein, EB1, is required for formation of polarized morphology and motility of melanoma cells. EB1 depletion decreased lamellipodia protrusion, and resulted in loss of opposed protruding and retracting cell edges. Lamellipodia attenuation correlated with mis-localization of filopodia throughout the cell and decreased Arp3 localization. EB1-depleted cells displayed less persistent migration and reduced velocity in single-cell motility experiments. We propose EB1 coordinates melanoma cell migration through regulating the balance between lamellipodial and filopodial protrusion.

1. Introduction

Cell motility is a complex process requiring coordinated re-organization of actin and microtubule cytoskeletons in both physiological and pathological conditions including angiogenesis and tumor cell metastasis. Filopodia and lamellipodia are protrusive structures localized to the cell front during motility [1], the activity of which is coordinated with trailing edge release from adhesive substrate [2]. These protrusive structures are regulated through the signaling molecules RhoA, Rac and Cdc42, and regulators of actin network organization including factors promoting actin filament nucleation and bundling [3-5]. Microtubules cooperate with the actin cytoskeleton to maintain cell polarization at leading and trailing edges during cell migration, and to remodel adhesive contacts with extracellular matrix protein [6,7]. Function of microtubules are controlled or mediated through microtubule plus-end tracking proteins [8] which bind preferentially to the growing microtubule plus-ends [9].

Polymerization of microtubules into the cell cortex place plus-end tracking proteins in a spatial context for mediating cross-talk with the protrusive actin cytoskeleton. A major group of plus-end tracking proteins is the EB1 family, comprised of human members with representative homologs in yeast and other organisms [10]. The N-terminus of EB1 protein contains a calponin homology domain that mediates binding to microtubules [11] followed by a coiled-coil domain responsible for dimerization [12]. EB1 proteins are known to control specific microtubule dynamic parameters. For example, EB1 promotes microtubule growth through increased rescue frequency and decreased catastrophe of plus-ends [13,14]. Yeast homologues of EB1 increase dynamic behavior of microtubules and decrease pausing of microtubule growth [15,16]. EB1 interacts with other plus-end tracking proteins [8] and controls accumulation of cytoplasmic linker proteins to microtubule ends [17].

EB1 was initially described as a binding partner of adenomatous polyposis coli (APC) [18], a tumor suppressor factor associated with colorectal cancer [19]. The EB1 C-terminal domain is

responsible for binding the C-terminal domain of APC [20]. Most of the APC mutations associated with colorectal cancer result in protein truncation [21], and thereby loss of EB1 interaction. EB1 is differentially expressed in various types of tumors and is associated with malignant phenotype. EB1 expression is increased in patient samples and cell lines from hepatocellular [22], esophageal [23], and human gastric [24] carcinomas; however, EB1 is decreased in pediatric ependymomas [25]. EB1 overexpression promotes cellular growth, activation of the beta-catenin/T-cell factor pathway and increases tumor formation [23,26]. Here we address the role of EB1 protein in actin protrusion dynamics and motility in mouse melanoma cells.

2. Materials and Methods

2.1 Cell culture and reagents

B16F1 mouse melanoma cells were purchased from American Type Culture Collection, Manassas, VA, USA and maintained in DMEM (Gibco Invitrogen, Carlsbad, CA, USA) supplemented with 10% fetal bovine serum (Atlanta Biologicals, Lawrenceville, GA, USA) and antibiotics. Trypsin/EDTA solution (Mediatech, Manassas, VA, USA) was used for cell detachment. Cells were transfected using Fugene 6 reagent according to manufacture protocol (Roche Diagnostics). Phalloidin conjugated to Alexa Fluor 350 was from Molecular Probes Invitrogen; rabbit affinity purified anti-Arp3 was from Millipore Corporation; mouse anti-fascin was from Santa Cruz Biotechnology, Inc, and mouse anti-EB1 was from BD Transduction Laboratories. TRITC-conjugated anti-mouse antibodies were from Jackson ImmunoResearch Laboratories; Alexa Fluor 488- conjugated anti-mouse and Alexa Fluor 647-conjugated anti-rabbit were from Molecular Probes Invitrogen.

2.2 RNA interference

The target sequence used for knock down of EB1 protein expression was GCCTGGACCAGCAGAGCAA (EB1 KD) and the two-nucleotide mismatch control sequence was GCCTGGACAAGCAGGGCAA (MM control). The target and MM control sequences were inserted into pGShin vector [27] and B16F1 cells were transfected using Fugene 6 reagent according to the manufacturer instructions. Experiments were performed 3 days after addition of vector when EB1 depletion averaged 92% in the transfected cell population identified by GFP co-expression [28].

2.3 Immunofluorescence microscopy

B16F1 cells transfected with EB1 or two-nucleotide mismatch control (MM control) shRNA constructs were plated onto glass coverslips coated with 30µg/ml mouse laminin (Invitrogen) for 24 hours at 4ºC and blocked with 2% bovine serum albumin. High refractive-index coverslips (Optical Analysis Corporation, Nashua, NH, USA) were used for total internal reflection fluorescence studies. For phalloidin staining, samples were fixed in phosphate-buffered saline (PBS) containing 1% glutaraldehyde and 0.5% Triton-X 100 for 20 minutes at room temperature. For EB1, fascin and Arp3 immunostaining cells were fixed in -20ºC methanol followed by post-fixation with 4% formaldehyde in PBS containing 0.1% Triton-X 100 for 10 minutes. Coverslips were mounted with Aqua poly/mount (Polysciences, Warrington, PA, USA). Total interval reflection fluorescence microscopy was performed on an Olympus IX70 inverted microscope equipped with an Apo 100X, 1.65 NA oil immersion objective and a 12-bit depth cooled CCD camera. All other fluorescence images were acquired using a Nikon Eclipse TE200 and Leica DMIRE2 HC microscopes fitted with 16-bit CCD cameras. For analysis of cell spreading and roundness index, threshold was applied to digital images of phalloidin fluorescence using Metamorph imaging software (Universal Imaging, Westchester, PA,

USA). The pixel areas of the objects (cells) created from the threshold images were converted to μm^2. The roundness index is the measured cell area divided by the area of a circle with a diameter equal to the longest chord through the cell. Line scan intensity analysis over the cell edge was performed on 16-bit images using Metamorph software. Z-series images were acquired at 0.5 μm-increments, deconvolved to reduce out-of-focus fluorescence and reconstructed using Metamorph. For presentation, images were rescaled and converted to 8-bit depth using Adobe Photoshop (Adobe Systems, Mountain View, CA, USA).

2.4 Live cell imaging and motility assay.

B16F1 cell spreading and single cell motility experiments were performed using the Delta T temperature control dish system (Bioptechs, Butler, PA, USA). Humidified air with 5% $CO2$ was infused into the enclosed system and temperature was maintained at 37ºC using the heated dish and lid system regulated by the Delta T4 controller (Bioptechs). Phase contrast images were acquired with a Leica DMIRE2 HC inverted microscope using 10X or 20X phase objectives. Cells were plated onto laminin at low density and images were acquired every 2.5 minutes for 78 minutes for analysis of cell edge protrusion and every 30 minutes for 22.5 hours for analysis of cell body displacement. For determination of cell edge protrusion velocity, kymographs were constructed and analyzed using Metamorph software. Protrusion velocity was taken as edge displacement in microns during the first 30 minutes of cell spreading. Cell migration was taken as displacement of the nucleus center in microns over 22.5 hours. Threshold for nucleus displacement was 1.7 μm. Average velocities over 22.5 hours for multiple cells were determined by linear regression analysis.

3. Results

3.1 EB1 knock down delays cell spreading and alters cell shape change.

We transfected B16F1 mouse melanoma cells with a plasmid encoding a short hairpin RNA (shRNA) sequence specific for EB1 or a two-nucleotide mismatch control sequence. Co-expression of soluble GFP allowed identification of transfected cells [27]. We achieved 92% depletion of EB1 protein in GFP-positive B16F1 cells as assessed by quantitative immunofluorescence on microtubule plus-ends [28]. Cells expressing EB1 knock down (EB1 KD) or two-nucleotide mismatch control (MM control) constructs were plated onto laminin, and fixed after 0.5, 1.0, 2.0 or 4.0 hours for assessment of cell spreading and polarization (Figure 1A). Roundness index, a measure of polarized cell morphology, was expressed as the ratio of projected cell area to the area of a circle with a diameter of the longest cord through the cell. Thus, a circular cell has a roundness index of 1.0 and a highly elongated cell approaching 0. Depletion of EB1 resulted in decreased cell area for up to 2.0 hours compared to cells expressing MM control sequence suggesting EB1 protein is involved in the rate of cell spreading (Figure 1B). Furthermore, EB1 depleted cells maintained circular shape over the whole time course, whereas cells expressing MM control shRNA and non-transfected cells underwent transition from circular to elongated shape (Figure 1A, C) suggesting EB1 protein is required for formation of polarized cell morphology. The loss of cell polarization in EB1 depleted cells may therefore correlate with defects in migration.

3.2 Depletion of EB1 decreases net protrusion and slows motility.

We next evaluated the effect of EB1 depletion on lamellipodia protrusion using phase contrast imaging of live cells. The analysis was performed for 78.0 minutes during which MM control and control cells spread uniformly for a period of 20-30 minutes followed by formation of distinct

protruding and retracting edges (Figure 2A, B). By contrast, EB1 depleted cells failed to form opposed protruding and retracting edges (Figure 2C). When dynamics of lamellipodia were analyzed using kymographs (Figure 2D), velocity of the advancing edge was significantly decreased in EB1 knock down cells consistent with the decreased cell area shown in Figure 1. The average velocity of edge protrusion was decreased by nearly 50% in EB1 depleted cells compared to controls (Table I). These data suggest that EB1 may positively regulate lamellipodia formation.

Study using a single-cell motility assay addressed the role of EB1 in cell migration. We tracked 2-dimensional translocation of individual cells on laminin for a period of approximately 24 hours. Figure 3A shows individual tracks in microns of non-transfected, EB1 KD and MM control cells. Motility of the EB1 depleted cell was substantially reduced compared to the cell expressing MM control shRNA and the non-transfected cell. Movement of multiple cells was averaged and converted to plots of cumulative distance traveled (Figure 3B) and distance from cell origin (Figure 3C). Average cell body velocity and distance from origin of EB1 KD cells was decreased approximately 40% and 70%, respectively, compared to MM control (Table I).

3.3 Enhanced filopodia and attenuated lamellipodia formation in EB1 depleted cells.

We examined whether disrupted actin protrusive activity in EB1 KD knock down cells was accompanied by imbalance between lamellipodia and filopodia formation. We used immunofluorescence staining of fascin, a marker of filopodia [29], and Arp3, a marker of lamellipodia [30] to determine localization and abundance of these structures. We found filopodia localized to what appeared to be the ventral surface of EB1 KD cells, whereas filopodia were restricted to the periphery in non-transfected cells (Figure 4A). The average number of filopodia per cell was increased at least two-fold in EB1 KD cells compared to non-transfected cells in the same (Figure 4B) or independent culture

(11.2 +/- 3.8 filopodia/cell at 30 minutes, n=19 cells). To confirm whether the filopodia in EB1 KD cells were projected from the ventral surface we used total internal reflection fluorescence (TIRF) microscopy [31]. The majority of the fascin-positive structures observed by wide field were also visible by TIRF microscopy (Figure 4C), indicating abnormal filopodia localization at the ventral surface in cells depleted of EB1. Acquisition of z-series through EB1 KD cells shows fascin-positive structures throughout the entire z-axis (Figure 4D). Arp3 was concentrated at the cell edge in both non-transfected and MM control cells; however, Arp3 fluorescence signal was significantly attenuated in EB1 depleted cells (Figure 5A). Line scan analysis over the cell edge demonstrated that Arp3 accumulation was decreased by approximately 50% in EB1 depleted cells compared to non-transfected and MM control cells (Figure 5B, C). These results show depletion of EB1 in melanoma cells causes increased production of filopodia and mis-localization of filopodia throughout the cell surface accompanied by down regulation of protrusive lamellipodia marked by Arp3 protein.

4. Discussion

EB1 protein is over expressed in several types of carcinoma [22-24] and binds to the C-terminal domain APC [20]. Since most of the mutations in APC associated with malignancy result in C-terminal truncation, binding with EB1 is lost raising the possibility that this interaction is an important part of the tumor suppressor function of APC.   APC knock down and domain truncation interfere with cell migration, protrusion and stabilization of microtubules [32].   Furthermore, APC interaction with microtubules and EB1 is important for microtubule stabilization and cell protrusive activities [32,33]. Our results show that depletion of EB1 protein interferes with net lamellipodial protrusion and cell body translocation. The effect of EB1 knock down on cell migration is likely the result of inability of cells to spatially regulate intracellular signaling events needed for polarization. Another striking feature of the

9

knock down cells is increased number and mis-localization of filopodia. In fibroblasts and B16F1 cells, Arp2/3 is normally excluded from filopodia [34], reflecting the fundamental difference between the molecular machinery of lamellipodia and filopodia protrusion. Cell movement requires optimal balance between these two modes of protrusion which is variable among cell types. For example, growth cones contain high density of filopodia [35], while fish keratocytes are devoid of filopodia [36]. B16F1 cell motility is intermediate, displaying both filopodia and lamellipodia modes of protrusion [1]. Shift in the balance can result in significant decrease in net protrusion [37]. Our results show EB1 is required to maintain balance between formation of lamellipodia and filopodia. Depletion of EB1 shifts the balance in favor of filopodial protrusion which likely interferes with overall cell body migration. The signaling mechanism of this regulation remains unclear. EB1 may control actin dynamics through regulation of fascin and Arp activity. For example, EB1 may regulate filopodia formation through altering fascin phosphorylation by protein kinase C [38,39] or regulate activity of Arp2/3 complex at lamellipodia protrusions [40]. In this regard, EB1 may control lamellipodia formation through regulation of microtubule-dependent transport of WAVE2 to cell protrusions [41,42]. Fascin expression is increased in various carcinomas [43] and Arp 2/3 expression correlates with invasiveness of colorectal tumor cells [44] and progression of gastric carcinoma [45]. Our current study combined with these published reports raise the intriguing possibility that EB1 regulates activity of fascin and Arp3 in a cell motility signaling pathway controlling melanoma metastasis.

Acknowledgements

Conflicts of interest statement

No conflicts of interest to disclose.

Fig. 1. EB1 knock down delays cell spreading and alters cell shape change. (A) B16F1 cells transfected with EB1 (EB1 KD) or mismatch sequence (MM control) shRNA constructs were plated onto laminin for the times indicated and were stained with Alexa Fluor 350-phalloidin (red). GFP (green) identifies cells transfected with shRNA constructs. Scale bar: 40 μm. (B) Plot of change in projected area of cells expressing EB1 KD or MM control shRNA, and non-transfected (control) cells. (C) Plot of change in shape (roundness index) of EB1 knockdown and control cells. EB1 knockdown cells maintain a non-polarized shape over 4 hours (*p<0.05, **p<0.01 unpaired t-test comparing EB1 KD to MM control). Error bars: SEM

Fig. 2. EB1 knock down interferes with formation of protruding and retracting cell edges. Representative time-lapse sequences of B16F1 cells transfected with MM control (A), non-transfected cells (B) and cells transfected with EB1 KD (C). GFP fluorescence is shown. (D) Kymograph analysis along the line (indicated at 0.0 minutes) of corresponding cells shown in A, B and C. Arrowheads and asterisks indicate protrusive and retracting edges, respectively. Kymographs were traced for clarity. Cell edge protrusion velocities obtained from kymographs are presented in Table I. Scale bar: 30 µm.

Fig. 3. EB1 knock down slows B16F1 cell migration. (A) Representative tracks of individual non-transfected (control), MM control and EB1 KD cells at 30-minute time intervals over 22.5 hours. Cumulative distance traveled (B) and the distance from origin (C) of multiple cells. Average cell body velocities and final displacements from origin are presented in Table I. Error bars: SEM (n=11 cells non-transfected and EB1 KD; n=8 cells MM control).

Fig. 4. Distribution of fascin in EB1 knock down cells. (A) Distribution of fascin immunofluorescence in EB1 KD and non-transfected cells on laminin for the times indicated. EB1 KD cells (asterisks) are identified by negative immunofluorescence staining for EB1 (not shown). Insets show enlarged regions of fascin staining in EB1 KD cells. Arrowheads indicate normal localization of fascin at the periphery of non-transfected cells. Scale bar: 40 µm. (B) Number of fascin-positive structures per cell for EB1 KD, MM control and non-transfected (control) cells (n=14-20 cells/bar). **p<0.01 unpaired t-test compared to MM control and non-transfected cells, error bars: SEM. (C) Representative wide field and total internal reflection fluorescence (TIRF) images of fascin in EB1 KD cells after 30 minutes on laminin. Scale bar: 10 µm. (D) Z-axis distribution of fascin immunofluorescence in EB1 KD, MM control and non-transfected cells (control) cells. Scale bar: 2 µm.

Fig. 5. Distribution of Arp3 in EB1 knockdown cells. (A) Arp3 immunofluorescence of representative EB1 KD, MM control and non-transfected cells at 0.5 hours. Asterisks indicate cells transfected with EB1 KD or MM control shRNA. Arrowheads indicate position of linescan over cell edge. Scale bar: 40 µm. (B) 13-micron linescan of Arp3 immunofluorescence intensity (arbitrary units) over edge of MM control (MM), non-transfected (Control) and EB1 knock down (EB1 KD) cells in Panel A. (C) Average Arp3 fluorescence intensity (arbitrary units) over edge of multiple cells (**$p<0.01$ unpaired t-test compared to MM control and control, n = 8-10 cells in each group, error bars: SEM).
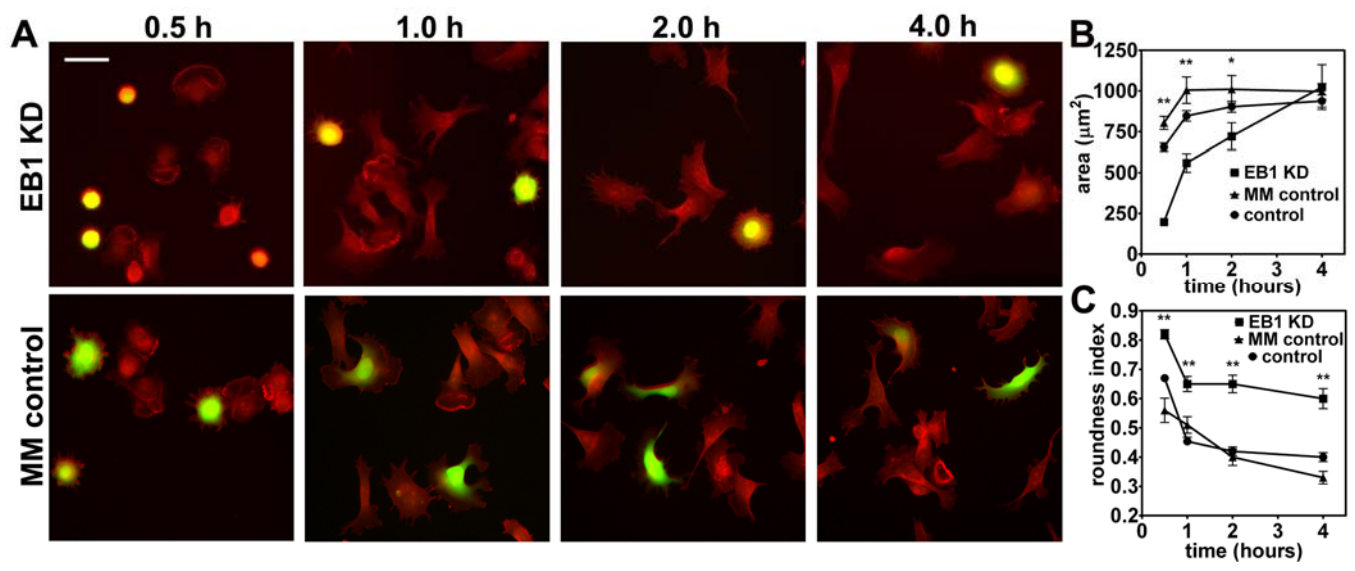
References

[1] J.V. Small, T. Stradal, E. Vignal, and K. Rottner, The lamellipodium: where motility begins, Trends Cell Biol. 12 (2002) 112-20.

[2] A.J. Ridley, M.A. Schwartz, K. Burridge, R.A. Firtel, M.H. Ginsberg, G. Borisy, J.T. Parsons, and A.R. Horwitz, Cell migration: integrating signals from front to back, Science 302 (2003) 1704-9.

[3] D. Yamazaki, S. Kurisu, and T. Takenawa, Regulation of cancer cell motility through actin reorganization, Cancer Sci. 96 (2005) 379-86.

[4] J.C. Adams, Roles of fascin in cell adhesion and motility, Curr. Opin. Cell Biol. 16 (2004) 590-6.

[5] E.D. Goley, and M.D. Welch, The ARP2/3 complex: an actin nucleator comes of age, Nat. Rev. Mol. Cell Biol. 7 (2006) 713-26.

[6] O.C. Rodriguez, A.W. Schaefer, C.A. Mandato, P. Forscher, W.M. Bement, and C.M. Waterman-Storer, Conserved microtubule-actin interactions in cell movement and morphogenesis, Nat. Cell Biol. 5 (2003) 599-609.

[7] J.V. Small, and I. Kaverina, Microtubules meet substrate adhesions to arrange cell polarity, Curr. Opin. Cell Biol. 15 (2003) 40-7.

[8] A. Akhmanova, and M.O. Steinmetz, Tracking the ends: a dynamic protein network controls the fate of microtubule tips, Nat. Rev. Mol. Cell Biol. 9 (2008) 309-22.

[9] P. Carvalho, J.S. Tirnauer, and D. Pellman, Surfing on microtubule ends, Trends Cell Biol. 13 (2003) 229-37.

[10] J.S. Tirnauer, and B.E. Bierer, EB1 proteins regulate microtubule dynamics, cell polarity, and chromosome stability, J. Cell Biol. 149 (2000) 761-6.

[11] I. Hayashi, and M. Ikura, Crystal structure of the amino-terminal microtubule-binding domain of end-binding protein 1 (EB1), J. Biol. Chem. 278 (2003) 36430-4.
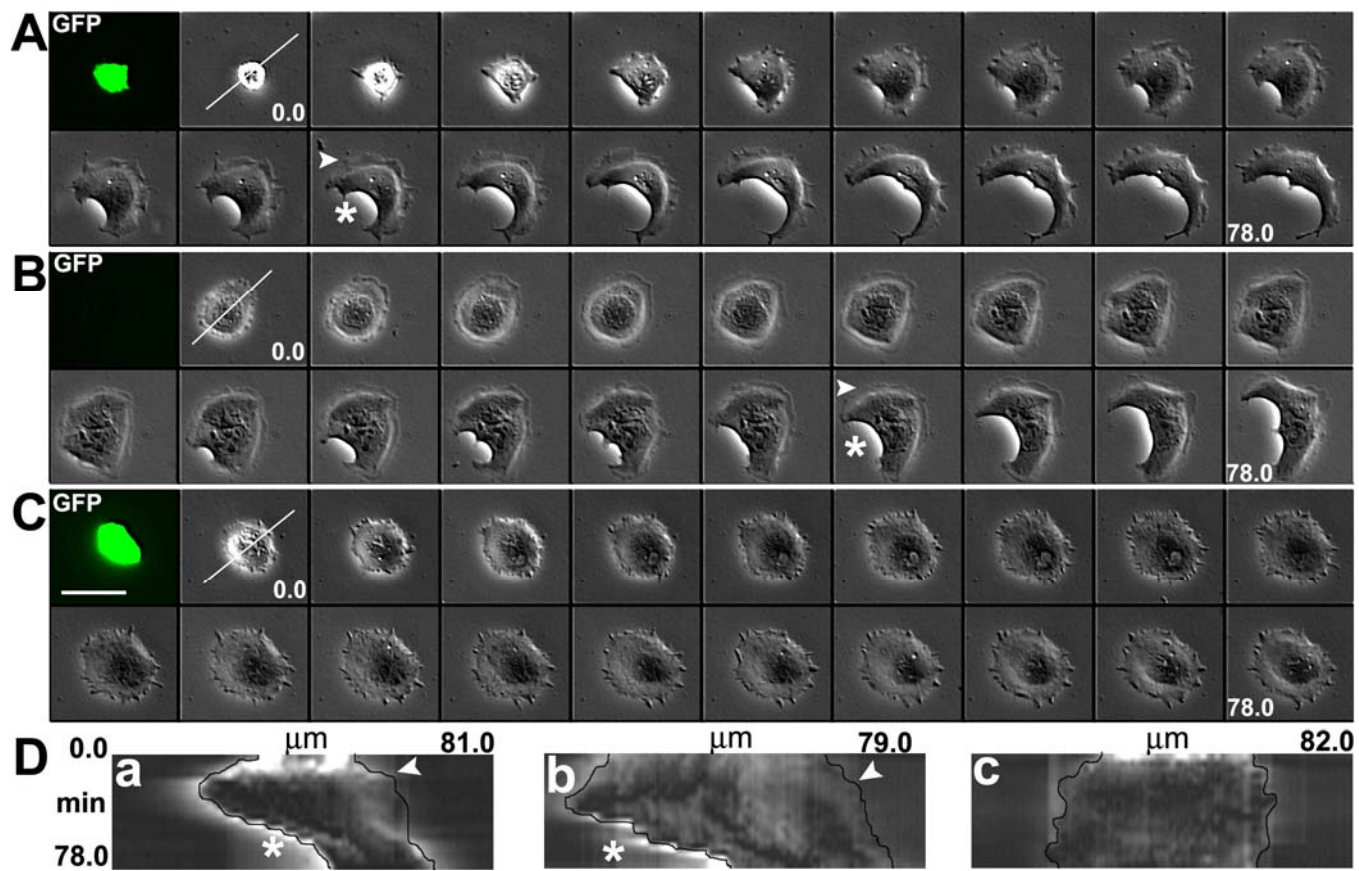
[12] M. Rehberg, and R. Graf, Dictyostelium EB1 is a genuine centrosomal component required for proper spindle formation, Mol. Biol. Cell 13 (2002) 2301-10.

[13] J.S. Tirnauer, S. Grego, E.D. Salmon, and T.J. Mitchison, EB1-microtubule interactions in Xenopus egg extracts: role of EB1 in microtubule stabilization and mechanisms of targeting to microtubules, Mol. Biol. Cell 13 (2002) 3614-26.

[14] Y. Komarova, C.O. De Groot, I. Grigoriev, S.M. Gouveia, E.L. Munteanu, J.M. Schober, S. Honnappa, R.M. Buey, C.C. Hoogenraad, M. Dogterom, G.G. Borisy, M.O. Steinmetz, and A. Akhmanova, Mammalian end binding proteins control persistent microtubule growth, J. Cell Biol. 184 (2009) 691-706.

[15] J.S. Tirnauer, E. O'Toole, L. Berrueta, B.E. Bierer, and D. Pellman, Yeast Bim1p promotes the G1-specific dynamics of microtubules, J. Cell Biol. 145 (1999) 993-1007.

[16] M.J. Wolyniak, K. Blake-Hodek, K. Kosco, E. Hwang, L. You, and T.C. Huffaker, The regulation of microtubule dynamics in Saccharomyces cerevisiae by three interacting plus-end tracking proteins, Mol. Biol. Cell 17 (2006) 2789-98.

[17] Y. Komarova, G. Lansbergen, N. Galjart, F. Grosveld, G.G. Borisy, and A. Akhmanova, EB1 and EB3 control CLIP dissociation from the ends of growing microtubules, Mol. Biol. Cell 16 (2005) 5334-45.

[18] L.K. Su, M. Burrell, D.E. Hill, J. Gyuris, R. Brent, R. Wiltshire, J. Trent, B. Vogelstein, and K.W. Kinzler, APC binds to the novel protein EB1, Cancer Res. 55 (1995) 2972-7.

[19] R. Fodde, The APC gene in colorectal cancer, Eur. J. Cancer 38 (2002) 867-71.

[20] S. Honnappa, C.M. John, D. Kostrewa, F.K. Winkler, and M.O. Steinmetz, Structural insights into the EB1-APC interaction, Embo J. 24 (2005) 261-9.

[21] Y. Miyoshi, H. Nagase, H. Ando, A. Horii, S. Ichii, S. Nakatsuru, T. Aoki, Y. Miki, T. Mori, and Y. Nakamura, Somatic mutations of the APC gene in colorectal tumors: mutation cluster region in the APC gene, Hum. Mol. Genet. 1 (1992) 229-33.

[22] K. Fujii, T. Kondo, H. Yokoo, T. Yamada, K. Iwatsuki, and S. Hirohashi, Proteomic study of human hepatocellular carcinoma using two-dimensional difference gel electrophoresis with saturation cysteine dye, Proteomics 5 (2005) 1411-22.
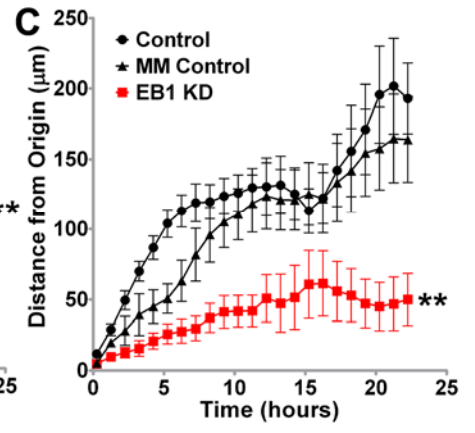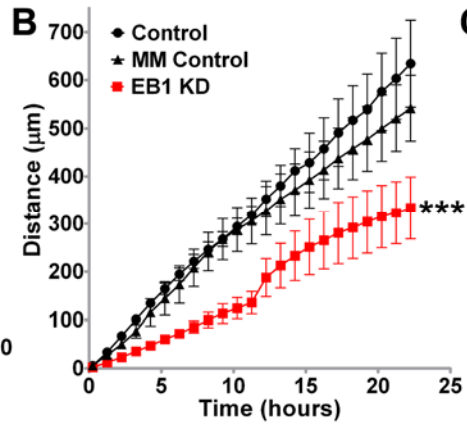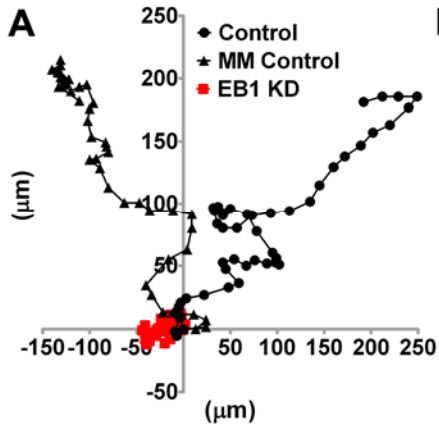
[23] Y. Wang, X. Zhou, H. Zhu, S. Liu, C. Zhou, G. Zhang, L. Xue, N. Lu, L. Quan, J. Bai, Q. Zhan, and N. Xu, Overexpression of EB1 in human esophageal squamous cell carcinoma (ESCC) may promote cellular growth by activating beta-catenin/TCF pathway, Oncogene 24 (2005) 6637-45.

[24] R. Nishigaki, M. Osaki, M. Hiratsuka, T. Toda, K. Murakami, K.T. Jeang, H. Ito, T. Inoue, and M. Oshimura, Proteomic identification of differentially-expressed genes in human gastric carcinomas, Proteomics 5 (2005) 3205-13.

[25] B. Suarez-Merino, M. Hubank, T. Revesz, W. Harkness, R. Hayward, D. Thompson, J.L. Darling, D.G. Thomas, and T.J. Warr, Microarray analysis of pediatric ependymoma identifies a cluster of 112 candidate genes including four transcripts at 22q12.1-q13.3, Neuro. Oncol. 7 (2005) 20-31.

[26] M. Liu, S. Yang, Y. Wang, H. Zhu, S. Yan, W. Zhang, L. Quan, J. Bai, and N. Xu, EB1 acts as an oncogene via activating beta-catenin/TCF pathway to promote cellular growth and inhibit apoptosis, Mol. Carcinog. (2008).

[27] S. Kojima, D. Vignjevic, and G.G. Borisy, Improved silencing vector co-expressing GFP and small hairpin RNA, Biotechniques 36 (2004) 74-9.

[28] J.M. Schober, Y.A. Komarova, O.Y. Chaga, A. Akhmanova, and G.G. Borisy, Microtubule-targeting-dependent reorganization of filopodia, J. Cell Sci. 120 (2007) 1235-44.

[29] D. Vignjevic, S. Kojima, Y. Aratyn, O. Danciu, T. Svitkina, and G.G. Borisy, Role of fascin in filopodial protrusion, J. Cell Biol. 174 (2006) 863-75.

[30] T.M. Svitkina, and G.G. Borisy, Arp2/3 complex and actin depolymerizing factor/cofilin in dendritic organization and treadmilling of actin filament array in lamellipodia, J. Cell Biol. 145 (1999) 1009-26.

[31] J.A. Steyer, and W. Almers, A real-time view of life within 100 nm of the plasma membrane, Nat. Rev. Mol. Cell Biol. 2 (2001) 268-75.

[32] K. Kroboth, I.P. Newton, K. Kita, D. Dikovskaya, J. Zumbrunn, C.M. Waterman-Storer, and I.S. Nathke, Lack of adenomatous polyposis coli protein correlates with a decrease in cell migration and overall changes in microtubule stability, Mol. Biol. Cell 18 (2007) 910-8.

[33] Y. Wen, C.H. Eng, J. Schmoranzer, N. Cabrera-Poch, E.J. Morris, M. Chen, B.J. Wallar, A.S. Alberts, and G.G. Gundersen, EB1 and APC bind to mDia to stabilize microtubules downstream of Rho and promote cell migration, Nat. Cell Biol. 6 (2004) 820-30.
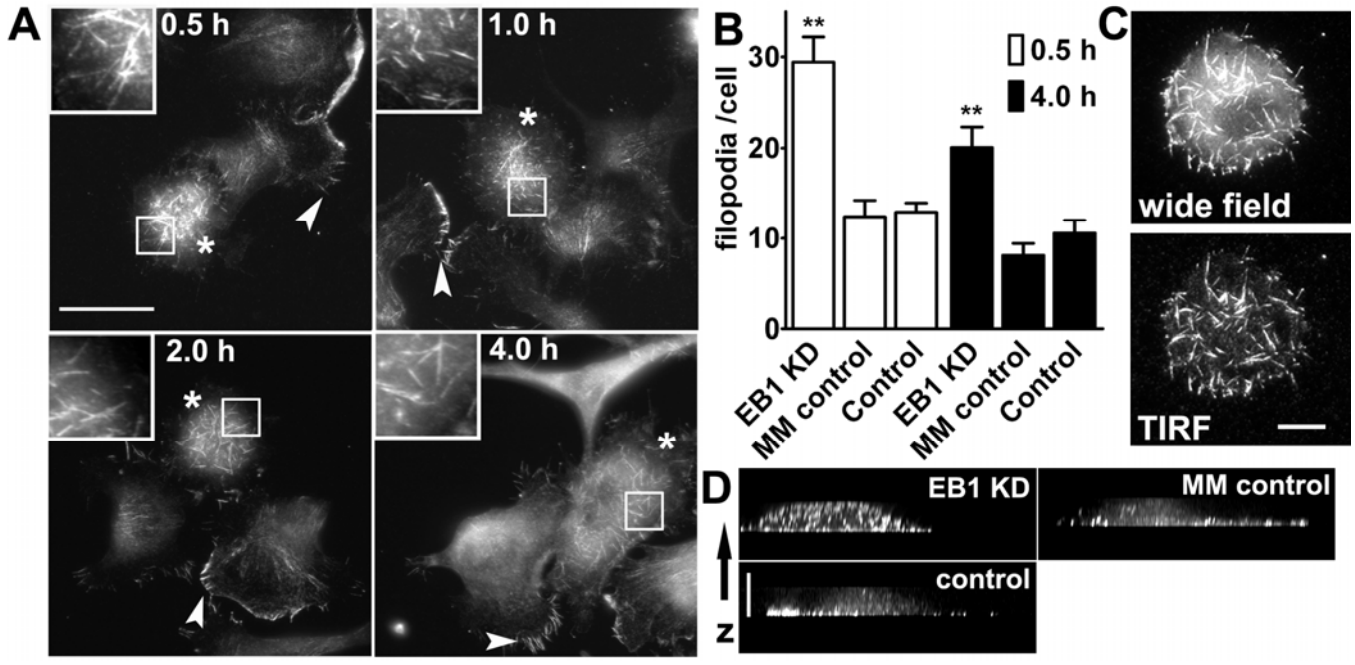
[34] T.M. Svitkina, E.A. Bulanova, O.Y. Chaga, D.M. Vignjevic, S. Kojima, J.M. Vasiliev, and G.G. Borisy, Mechanism of filopodia initiation by reorganization of a dendritic network, J. Cell Biol. 160 (2003) 409-21.

[35] A.W. Schaefer, N. Kabir, and P. Forscher, Filopodia and actin arcs guide the assembly and transport of two populations of microtubules with unique dynamic parameters in neuronal growth cones, J. Cell Biol. 158 (2002) 139-52.

[36] J.V. Small, M. Herzog, and K. Anderson, Actin filament organization in the fish keratocyte lamellipodium, J. Cell Biol. 129 (1995) 1275-86.

[37] M.R. Mejillano, S. Kojima, D.A. Applewhite, F.B. Gertler, T.M. Svitkina, and G.G. Borisy, Lamellipodial versus filopodial mode of the actin nanomachinery: pivotal role of the filament barbed end, Cell 118 (2004) 363-73.

[38] Y. Yamakita, S. Ono, F. Matsumura, and S. Yamashiro, Phosphorylation of human fascin inhibits its actin binding and bundling activities, J. Biol. Chem. 271 (1996) 12632-8.

[39] S. Ono, Y. Yamakita, S. Yamashiro, P.T. Matsudaira, J.R. Gnarra, T. Obinata, and F. Matsumura, Identification of an actin binding region and a protein kinase C phosphorylation site on human fascin, J. Biol. Chem. 272 (1997) 2527-33.

[40] C. Le Clainche, D. Schlaepfer, A. Ferrari, M. Klingauf, K. Grohmanova, A. Veligodskiy, D. Didry, D. Le, C. Egile, M.F. Carlier, and R. Kroschewski, IQGAP1 stimulates actin assembly through the N-WASP-Arp2/3 pathway, J. Biol. Chem. 282 (2007) 426-35.

[41] S. Kurisu, S. Suetsugu, D. Yamazaki, H. Yamaguchi, and T. Takenawa, Rac-WAVE2 signaling is involved in the invasive and metastatic phenotypes of murine melanoma cells, Oncogene 24 (2005) 1309-19.

[42] K. Takahashi, and K. Suzuki, Requirement of kinesin-mediated membrane transport of WAVE2 along microtubules for lamellipodia formation promoted by hepatocyte growth factor, Exp. Cell Res. 314 (2008) 2313-22.

[43] Y. Hashimoto, M. Skacel, and J.C. Adams, Roles of fascin in human carcinoma motility and signaling: prospects for a novel biomarker?, Int. J. Biochem. Cell Biol. 37 (2005) 1787-804.

[44] T. Otsubo, K. Iwaya, Y. Mukai, Y. Mizokami, H. Serizawa, T. Matsuoka, and K. Mukai, Involvement of Arp2/3 complex in the process of colorectal carcinogenesis, Mod. Pathol. 17 (2004) 461-7.

[45] H.C. Zheng, Y.S. Zheng, X.H. Li, H. Takahashi, T. Hara, S. Masuda, X.H. Yang, Y.F. Guan, and Y. Takano, Arp2/3 overexpression contributed to pathogenesis, growth and invasion of gastric carcinoma, Anticancer Res. 28 (2008) 2225-32.

A

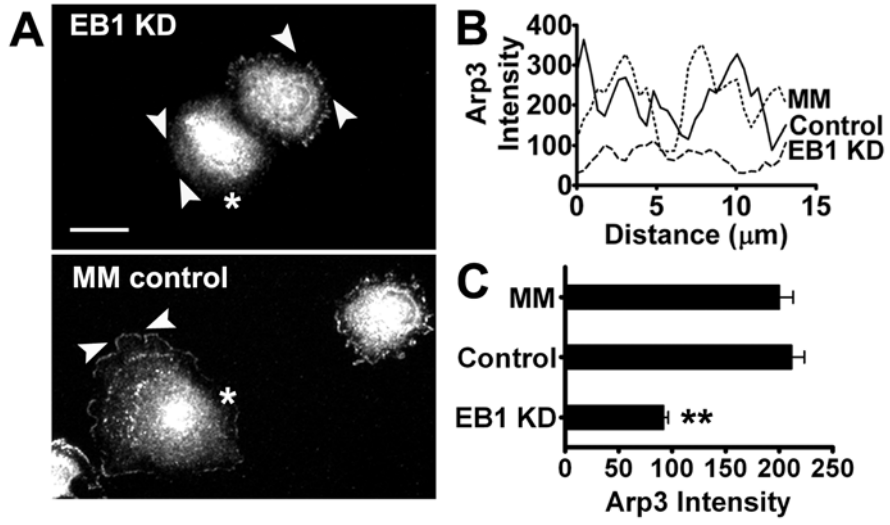|	0.5 h	1.0 h	2.0 h	4.0 h
EB1 KD				
MM control				

B

area (μm²) vs time (hours)
- EB1 KD
- MM control
- control

C

roundness index vs time (hours)
- EB1 KD
- MM control
- control

A EB1 KD

MM control

B

Arp3 Intensity vs Distance (μm)

MM
Control
EB1 KD

C

MM
Control
EB1 KD **

Arp3 Intensity

Table I. Cell Motility Parameters

Parameter	EB1 KD	MM Control	Control
Edge Protrusion[#] (µm/min +/- s.e.m.)	**0.27 +/- 0.02	0.52 +/- 0.06	0.47 +/- 0.04
Cell Body Velocity[†] (µm/hour +/- s.e.m.)	**15.2 +/- 0.30	25.5 +/- 0.27	28.6 +/- 0.12
Final Cell Displacement from Origin[‡] (µm +/- s.e.m.)	*50.1 +/- 12.3	164.0 +/- 30.4	193 .0 +/- 15.1

\# velocity of cell edge protrusion averaged over initial 30 minutes of spreading; † velocity of cell body displacement averaged over 22.5 hours; ‡ average of final cell body displacement from origin after migration for 22.5 hours; *$p < 0.01$ and **$p < 0.001$ EB1 KD compared to MM control and control; n = 11-12 cells